HHS Public Access

Author manuscript

*Inorg Chem*. Author manuscript; available in PMC 2017 June 06.

Published in final edited form as:

*Inorg Chem*. 2016 June 6; 55(11): 5467–5475. doi:10.1021/acs.inorgchem.6b00491.

# Synthesis, Radical Reactivity, and Thermochemistry of Monomeric Cu(II) Alkoxide Complexes Relevant to Cu/Radical Alcohol Oxidation Catalysis

**Thomas R. Porter**[‡], **Dany Capitao**[‡], **Werner Kaminsky**, **Zhaoshen Qian**, and **James M. Mayer**[*,§]

Department of Chemistry, University of Washington, Box 351700, Seattle, Washington 98195, United States

## Abstract

Two new monomeric Cu(II) alkoxide complexes were prepared and fully characterized as models for intermediates in copper/radical mediated alcohol oxidation catalysis: $Tp^{tBuR}Cu^{II}OCH_2CF_3$ with $Tp^{tBu}$ = hydro-tris(3-*tert*-butyl-pyrazol-1-yl)borate **1** or $Tp^{tBuMe}$ = hydro-tris(3-*tert*-butyl-5-methylpyrazol-1-yl)borate **2**. These complexes were made as models for potential intermediates in enzymatic and synthetic catalytic cycles for alcohol oxidation. However, the alkoxide ligands are not readily oxidized by loss of H; instead, these complexes were found to be hydrogen atom *acceptors*. They oxidize the hydroxylamine TEMPOH, 2,4,6-tri-*t*-butylphenol, and 1,4-cyclohexadiene to the nitroxyl radical, phenoxyl radical, and benzene, with formation of $HOCH_2CF_3$ (TFE) and the Cu(I) complexes $Tp^{tBuR}Cu^{I}MeCN$ in dichloromethane/1% MeCN or 1/2 $[Tp^{tBuR}Cu^{I}]_2$ in toluene. On the basis of thermodynamics and kinetics arguments, these reactions likely proceed through concerted proton–electron transfer mechanisms. Thermochemical analyses give lower limits for the "effective bond dissociation free energies (BDFE)" of the O–H bonds in $1/2[Tp^{tBuR}Cu^{I}]_2$ + TFE and upper limits for the free energies associated with alkoxide oxidations via hydrogen atom transfer (*effective* alkoxide α-C–H BDFEs). These values are summations of the free energies of multiple chemical steps, which include the energetically favorable formation of $1/2[Tp^{tBuR}Cu^{I}]_2$. The *effective* alkoxide α-C–H bonds are very weak, BDFE ≤ 38 ± 4 kcal $mol^{-1}$ for **1** and ≤44 ± 5 kcal $mol^{-1}$ for **2** (gas-phase estimates), because C–H homolysis is thermodynamically coupled to one electron transfer to Cu(II) as well as the favorable

[*]**Corresponding Author**. James.mayer@yale.edu.

[‡](T.R.P. and D.C.) Laboratoire d'Electrochimie Moléculaire, Université Paris Diderot, 15 Rue Jean-Antoine de Baïf, F-75205 Paris Cedex 13, France.

[§](J.M.M.) Department of Chemistry, Yale University, 225 Prospect St., New Haven, CT 06520, United States.

**ASSOCIATED CONTENT**

**Supporting Information**

The Supporting Information is available free of charge on the ACS Publications website at DOI: 10.1021/acs.inorgchem.6b00491.

Crystallographic information, additional NMR and optical characterization, EPR spectra, cyclic voltammograms, reaction characterization, thermochemical conversions, computational details. (PDF)

X-ray crystallographic information. (CIF)

X-ray crystallographic information. (CIF)

X-ray crystallographic information. (CIF)

The authors declare no competing financial interest.

formation of the 1/2[Tp$^{tBuR}$Cu$^{I}$]$_2$ dimer. Treating **1** with the H atom acceptor $^{t}$Bu$_3$ArO$^{\bullet}$ did not result in the expected alkoxide oxidation to an aldehyde, but rather net 2,2,2-trifluoroethoxyl radical transfer occurred to generate an unusual 2-substituted dienone–ether product. Treating **2** with $^{t}$Bu$_3$ArO$^{\bullet}$ gives no reaction, despite evidence that overall ligand oxidation and formation of 1/2[Tp$^{tBuMe}$Cu$^{I}$]$_2$ is significantly exoergic. The origin of this lack of reactivity may be due to insufficient weakening of the alcohol α-C–H bond upon complexation to copper.

## Graphical abstract

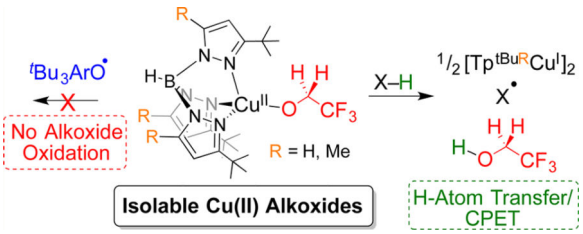


## INTRODUCTION

Copper/radical mediated alcohol oxidation has been studied extensively in biological[1] and synthetic organic systems.[2] In these systems, the $2H^{+}/2e^{-}$ oxidation of an alcohol to an aldehyde or ketone is achieved by utilizing the oxidizing equivalents from Cu(II) and an oxyl radical. In biology, this reaction is performed by the fungal enzyme, galactose oxidase. Galactose oxidase performs this reaction with Cu(II) and an anti-ferromagnetically coupled tyrosine-derived oxyl radical.[1] In synthetic organic applications, alcohol oxidation is typically achieved with the use of an $L_nCu^{II}$ complex and a nitroxyl radical such as 2,2,6,6-tetramethylpiperidine-*N*-oxyl (TEMPO) or 9-azobicyclo[3.3.1]nonane *N*-oxyl (ABNO).[2]

Both galactose oxidase and Cu/nitroxyl systems have been well studied, and catalytic schemes have been constructed for both. Various mechanisms have been proposed based on combinations of kinetics and computational results.[1,2] In both examples, the consensus mechanisms of alcohol oxidation involve the formation of a Cu(II) alkoxide intermediate through a protolytic ligand exchange pathway. The subsequent reaction in both cases involves the net transfer of one electron to Cu(II) and a hydrogen atom ($H^{+}/e^{-} \equiv H^{\bullet}$) from the α-C–H position of the alkoxide to the oxyl radical to give the corresponding aldehyde or ketone. This could occur by H atom transfer (HAT) to the oxygen of the oxyl radical, concerted with or prior to reduction of Cu(II) (Scheme 1). Recent computational studies have shown in one system that precoordination of the nitroxyl radical to Cu(II) facilitates a concerted $2e^{-}/H^{+}$ transfer reaction (Scheme 2).[2e]

Previous kinetics studies in both systems have shown that deuteration of the α-position of the alcohol substrate results in a large primary kinetic isotope effect (KIE), suggesting that hydrogen transfer is involved in the rate-determining step.[1i,2b] Cu(II) must be playing a substantial role in modulating the thermochemistry in this H transfer step, as typically the bond strength of the α-C–H bond in an alcohol is much stronger than the O–H bond formed by the oxyl radical.[3]

One of the challenges associated with studying these reactions is the difficulty in preparing simple monomeric Cu(II) alkoxide model complexes for stoichiometric reactivity studies. Most examples involve tertiary alkoxides,[4] highly fluorinated hexafluoroisopropoxides,[5] or special supporting ligands.[6]

We report here the preparation of monomeric Cu(II) alkoxide complexes including $Tp^{tBuR}Cu^{II}OCH_2CF_3$ with $Tp^{tBuR}$ = $Tp^{tBu}$ = hydro-tris(3-*tert*-butyl-pyrazol-1-yl)borate **1** or $Tp^{tBuMe}$ = hydro-tris(3-*tert*-butyl-5-methyl-pyrazol-1-yl)borate **2**. These compounds were inspired by $Tp^{R,R'}Cu^{II}$-X complexes ($Tp^{R,R'}$ = hydro-tris(3-R-5-R′-pyrazolylborate)) previously reported by Tolman[7] and others.[8–10] Complete characterization including $^1H$ NMR spectra and X-ray crystal structures indicates fluxional trigonal-monopyramidal structures. A companion article has already appeared,[11] describing single-crystal electron paramagnetic resonance (EPR) and electron nuclear double resonance (ENDOR) studies and indicating an unusual electronic structure.

Both **1** and **2** can *abstract* hydrogen atoms from weak O–H bonds, forming $HOCH_2CF_3$, the oxyl radical, and $1/2[Tp^{tBuR}Cu^{I}]_2$.[7c,8b] However, these compounds do not readily donate H atoms to oxyl radicals in the manner suggested in Scheme 1. Surprisingly, treatment of **1** with the 2,4,6-tri-*tert*-butylphenoxyl radical ($^tBu_3ArO^{\bullet}$) in toluene resulted in the net transfer of $^{\bullet}OCH_2CF_3$ to form an unusual nonaromatic diene-one product and $1/2[Tp^{tBu}Cu^{I}]_2$, without oxidation of the alkoxide. Complex **2** was unreactive with $^tBu_3ArO^{\bullet}$ under these conditions. Thus, neither **1** nor **2** undergo hydrogen atom transfer from the alkoxide ligand to an external phenoxyl radical, as suggested in Scheme 1. Thermochemical analysis indicates that the unobserved alkoxide oxidation reactions are overall highly exoergic. The origin of the kinetic barrier is discussed.

## RESULTS

### Preparation and Characterization of Cu(II) Alkoxides

Treatment of $Tp^{tBu}Cu^{II}OTf$[7a] in dichloromethane (DCM) with 1 equiv of 1,8-diazabicycloundec-7-ene (DBU) and a slight excess of 2,2,2-trifluoroethanol (TFE) yielded $Tp^{tBu}Cu^{II}OCH_2CF_3$ (**1**, eq 1). This was evident from the dramatic color change from deep purple to orange as well as the appearance of new paramagnetically shifted pyrazole resonances in the $^1H$ NMR spectrum of the reaction mixture. Recrystallization from saturated pentane solutions at −30 °C yields large red-orange crystals of **1**.

$$Tp^{tBu}Cu^{II}OTf + HOCH_2CF_3 + DBU \rightarrow Tp^{tBu}Cu^{II}OCH_2CF_3\,(\mathbf{1}) + [DBU{-}H^+][OTf^-] \quad (1)$$

The related complex, $Tp^{tBuMe}Cu^{II}OCH_2CF_3$ **2**, with the more sterically crowded 3-$^t$Bu-5-Me pyrazole-derived ligand, was prepared in the same manner. With the $Tp^{tBu}$ ligand, the related trifluoro-isopropoxide complex $Tp^{tBu}$Cu-OCH($CH_3$)$CF_3$ (complex **3**) was prepared similarly and fully characterized (see Supporting Information). The decomposition of **3** in solution over ca. 10 h made it less convenient for study.

The same synthetic protocol with the nonfluorinated alcohol EtOH led to a similar color change and NMR spectrum (Supporting Information). The product was tentatively assigned as the corresponding $Tp^{tBu}Cu^{II}OEt$ complex but could not be isolated due to its instability. $Tp^{tBu}Cu^{II}OEt$ decomposed to a complex mixture of products, including ethanol and a very small amount of acetaldehyde.

The X-ray structures of **1**, **2**, and **3** were found to contain similar four-coordinate copper complexes. They have trigonal monopyramidal geometries consisting of two short Cu–pyrazole N bonds and a short alkoxide Cu–O bond in the basal plane, with the third pyrazole nitrogen binding axially with a notably longer Cu–N bond (Figure 1, Table 1). The degree of geometric distortion from tetrahedral can be described quantitatively with the pyramidalization normalization parameter τ, which varies from 0 for a perfect tetrahedral to 1 for perfect trigonal monopyramidal.[12] The τ values for **1** and **2** were both 0.76, similar to the related cumylperoxide complex $Tp^{iPriPr}Cu^{II}OOCm$ ($Tp^{iPriPr}$ = hydro-tris(3,5-di-*iso*-propylpyrazolyl) borate).[9b,f] Complex **3** is slightly more tetrahedral (τ = 0.63), closer to $Tp^{tBu}Cu^{II}Cl$ and $Tp^{tBu}Cu^{II}OTf$ (τ = 0.47, 0.39; for a complete table, see Supporting Information).[7,8]

The X-band EPR spectra of both **1** and **2** in toluene glasses at 120 K display axial $g_{\|} > g_{\perp}$ signals (Figures 2, S7, and S8). The spectra are very similar to those observed for the structurally related Kitajima/Fujisawa complexes.[9a,c,f] In contrast, **3** has a rhombic signal more like those reported by Tolman for the more tetrahedral complexes.[7d] Initial fitting of the spectra yield, $g_{\|}$ = 2.44 (**1**)/2.43 (**2**), $|A_{\|}^{Cu}| = 40 \times 10^{-4}$ (**1**) $cm^{-1}/41 \times 10^{-4}$ $cm^{-1}$ (**2**), and $g_{\perp}$ = 2.07 (**1**)/2.07 (**2**). Like the Kitajima/Fujisawa examples, these $g_{\|}$ values are unusually large, and the $|A_{\|}^{Cu}|$ values are exceptionally small compared to what is typically observed for "normal" axial $g_{\|} > g_{\perp}$ Cu(II) EPR spectra (i.e., $[CuCl_4]^{2-}$ $g_{\|}$ = 2.221, $|A_{\|}^{Cu}| = 164 \times 10^{-4}$ $cm^{-1}$).[13] A much more detailed spectroscopic analysis of **1** has been reported separately.[11]

$^1$H NMR spectra of **1**–**3** show equivalent pyrazole signals indicating effective $C_{3v}$ symmetry (Figure 3), in contrast to the distortions found in the X-ray crystal structures and the EPR spectra. Thus, the molecules are fluxional on the NMR time scale. This NMR pattern is the same as was observed for a number of previously known $Tp^{R,R'}Cu^{II}X$ complexes, some of which had not been characterized by NMR previously (Table S5). These relatively sharp spectral features are very useful for characterization and monitoring reactions (vide infra).

## Electrochemistry and Acid/Base Properties

Cyclic voltammograms of **1**–**3** in $CH_2Cl_2$ with 0.1 M $[N^nBu_4][PF_6]$ and at 100 mV $s^{-1}$ display irreversible cathodic peak potentials at −0.86, −1.03, and −0.84 V, respectively (all ±0.01 V and vs $Fc^{+/0}$; Figure S10). Electrochemical irreversibility has previously been reported by Tolman for similar $Tp^{tBu}Cu$ complexes.[7c]

The basicity of **1** was examined. No reaction was observed between **1** or **2** and $[DBUH^+]$ $[^-OTf]$ in DCM-$d_2$/1% MeCN-$d_3$ (v/v). This is consistent with their syntheses (eq 1). (Unless otherwise noted, this solvent mixture and 15.3 mM copper concentrations were used

in all of the reaction chemistry reported here; the small amount of MeCN provides stability to the Cu(II) and Cu(I) products.) The stronger acid,[14] 2,6-lutidinium triflate [LutH$^+$][$^-$OTf], converts ca. 20% of **1** to [Tp$^{t\mathrm{Bu}}$Cu$^{\mathrm{II}}$(MeCN-$d_3$)$^+$]$^{7a,15}$ + HOCH$_2$CF$_3$ by $^1$H NMR, along with some minor side products. This indicates that the basicity of **1** is close to that of lutidine.

## Reactions with H-Atom Donors

The addition of 1 equiv of the hydrogen atom donor 2,2,6,6-tetramethylpiperdin-1-ol (TEMPO–H) to a solution of **1** resulted in an immediate color change from orange to light pink. The $^1$H NMR spectrum of the resulting solution showed quantitative yields of Tp$^{t\mathrm{Bu}}$Cu$^{\mathrm{I}}$(MeCN-$d_3$)[7c] and TFE (eq 2), based on integration versus a fluorobenzene internal standard, and disappearance of TEMPO–H. The TFE signal was also observed and quantified using $^{19}$F NMR spectroscopy. Thus, HAT has occurred from the potent H atom donor TEMPO–H (O–H bond dissociation free energy (BDFE$_{\mathrm{tol}}$) = 65.2 kcal mol$^{-1}$)[16] to **1**.

$$\mathrm{Tp}^{t\mathrm{Bu}}\mathrm{Cu}^{\mathrm{II}}\mathrm{OCH_2CF_3} + \mathrm{TEMPO{-}H} + \mathrm{MeCN}{-}d_3 \rightarrow \mathrm{Tp}^{t\mathrm{Bu}}\mathrm{Cu}^{\mathrm{I}}(\mathrm{MeCN}{-}d_3) + \mathrm{HOCH_2CF_3} + \mathrm{TEMPO} \quad (2)$$

The same reactivity is observed with the hydroxylamine 9-azabicyclo[3.3.1]nonane *N*-hydroxide (ABNO–H; O–H BDFE$_{\mathrm{tol}}$ = 70.7 kcal mol$^{-1}$).[17] In this case the nitroxyl radical product ABNO$^\bullet$ was detected and quantified with optical spectroscopy.

Similar reactions were observed between **1** and the phenolic hydrogen atom donors 2,4,6-tri-*tert*-butyl-phenol ($^t$Bu$_3$ArOH) and 2,6-di-*tert*-butyl-4-(4′-nitrophenyl)phenol ($^t$Bu$_2$NPArOH; eq 3). The Tp$^{t\mathrm{Bu}}$Cu$^{\mathrm{I}}$-MeCN-$d_3$ and TFE products were quantified by $^1$H NMR and $^{19}$F NMR spectroscopies. $^t$Bu$_3$ArO$^\bullet$ (2,4,6-tri-*tert*-butyl-phenoxyl radical)[18] and $^t$Bu$_2$NPArO$^\bullet$ (2,6-di-*tert*-butyl-4-(4′-nitrophenyl)phenoxyl radical)[19] were quantified from their optical spectra. These react more slowly than the hydroxylamines, requiring 3 and 8 h, respectively. This is presumably because they have stronger O–H bonds, as discussed below.

$$\mathrm{Tp}^{t\mathrm{Bu}}\mathrm{Cu}^{\mathrm{II}}\mathrm{OCH_2CF_3} + \mathrm{ArO{-}H} + \mathrm{MeCN}{-}d_3 \rightarrow \mathrm{Tp}^{t\mathrm{Bu}}\mathrm{Cu}^{\mathrm{I}}(\mathrm{MeCN}{-}d_3) + \mathrm{HOCH_2CF_3} + \mathrm{ArO}^\bullet \quad (3)$$

1,4-cyclohexadiene (1,4-CHD; first C–H BDFE$_{\mathrm{tol}}$ = 72.6 kcal mol$^{-1}$)[17] is also oxidized by **1**, forming benzene (eq 4). This reaction required over two weeks to reach completion even in the presence of 50-fold excess 1,4-CHD (**1** is stable over that time period in the absence of 1,4-CHD).

$$2\mathrm{Tp}^{t\mathrm{Bu}}\mathrm{Cu}^{\mathrm{II}}\text{–}\mathrm{OCH_2CF_3} + 1,4\text{–}\mathrm{CHD} + \mathrm{MeCN}\text{–}d_3 \rightarrow 2\mathrm{Tp}^{t\mathrm{Bu}}\mathrm{Cu}^{\mathrm{I}}\text{–}\mathrm{MeCN}\text{–}d_3 + \mathrm{HOCH_2CF_3} + \mathrm{C_6H_6} \quad (4)$$

Similar HAT reactivity was also observed for $\mathrm{Tp}^{t\mathrm{BuMe}}\mathrm{Cu}^{\mathrm{II}}$–$\mathrm{OCH_2CF_3}$ (**2**) in DCM-$d_2$/1% MeCN-$d_3$[20] but the reaction times were slightly longer relative to those of **1** (i.e., the reaction with $^t\mathrm{Bu_3ArO}$–H requires ~5 h for (**2**) and ~3 h for (**1**)).

In toluene-$d_8$ solutions both **1** and **2** were found to be slightly poorer hydrogen atom acceptors. Complex **1** quantitatively oxidized $^t\mathrm{Bu_3ArO}$–H, but only ~70% reacted with $^t\mathrm{Bu_2NPArO}$–H (eq 5). Likewise, **2** reacted quantitatively with ABNO–H, but only ~30% reacted with $^t\mathrm{Bu_3ArO}$–H. In these reactions, the absence of a ligand like MeCN, the product is the previously characterized[7c] Cu(I) dimer (eq 5).

$$\mathrm{Tp}^{t\mathrm{BuR}}\mathrm{Cu}^{\mathrm{II}}\text{–}\mathrm{OCH_2CF_3} + \mathrm{RO}\text{–}\mathrm{H} \rightarrow 1/2[\mathrm{Tp}^{t\mathrm{BuR}}\mathrm{Cu}^{\mathrm{I}}]_2 + \mathrm{RO}^{\bullet} + \mathrm{HOCH_2CF_3} \quad (5)$$

## Reactions with $^t\mathrm{Bu_3ArO}^{\bullet}$

Treatment of **1** with 1 equiv of $^t\mathrm{Bu_3ArO}^{\bullet}$ resulted in a solution color change from dark green (**1** is orange, $^t\mathrm{Bu_3ArO}^{\bullet}$ is blue) to light lime green over the course of ~10 h. The $^1$H NMR spectrum showed the appearance of $\mathrm{Tp}^{t\mathrm{Bu}}\mathrm{Cu}^{\mathrm{I}}$-MeCN-$d_3$ as well as quantitative formation of organic species **4**. $^1$H and $^{19}$F NMR studies identified **4** as the unusual 2,4-cyclohexadien-1-one, 2,4,6-tri*tert*-butyl-6-(2,2,2-trifluoroethoxide) (eq 6; see Supporting Information).

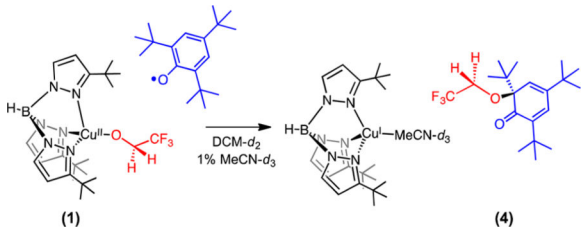


(6)

Compound **4** is formed, at least formally, by net transfer of a trifluoroethoxyl radical from copper to the ortho carbon of the phenoxyl radical. This reaction occurs both in DCM-$d_2$/1% MeCN-$d_3$ (v/v) and in toluene-$d_8$.

From the extensive Cu/radical alcohol oxidation literature,[1,2] we anticipated that $^t\mathrm{Bu_3ArO}^{\bullet}$ would oxidize the alkoxide ligand in **1** to give phenol and trifluoroacetaldehyde products (Scheme 1). However, these are not observed, nor is the corresponding phenol-trifluoroacetaldehyde hemiacetal ($CF_3CHO$ is a very reactive and electrophilic aldehyde). To test whether $CF_3CHO$ could be a reactive intermediate en route to **4**, a series of experiments was performed with the $\mathrm{Tp}^{t\mathrm{Bu}}\mathrm{Cu}^{\mathrm{II}}$–$\mathrm{OC\underline{D}_2CF_3}$ isotopologue, **1**-$d_2$.

Kinetics analysis of this reaction in DCM-$d_2$/1% MeCN-$d_3$ (v/v) under pseudo-first-order conditions showed a first-order dependence on $^t$Bu$_3$ArO$^\bullet$ but gave irreproducible second-order rate constants that varied between $7.2 \times 10^{-2}$ and $18.0 \times 10^{-2}$ $M^{-1}$ $s^{-1}$. The rate constants were generally consistent between runs only when the same stock solvent was used. In the same batch of solvent, **1** and **1**-$d_2$ reacted at the same rate within the ca. ±20% experimental uncertainty. The kinetic isotope effect of ca. 1 is evidence against H(D) transfer in the rate-determining step.

In a second experiment, a solution of 0.5 equiv of **1** and **1**-$d_2$ was combined with a full equivalent of $^t$Bu$_3$ArO$^\bullet$. Only **4** and **4**-$d_2$ were observed as products (by $^1$H NMR). If CF$_3$C(H/D)O were an intermediate, then the reaction would have formed the monodeuterated **4**-$d_1$ (Ar–OCHDCF$_3$), with a CHD methylene unit of trifluoroethoxy substituent (Scheme 3). This rules out the pathway of initial oxidation of the alkoxide ligand by the phenoxyl radical.

Density functional theory free energy calculations (rM06/6-311+g(d,p), gas phase, and toluene self-consistent reaction field (SCRF))[21] show that $^t$Bu$_3$CHDO-TFE is higher in energy than the sum of free energies of trifluoroacetaldehyde and $^t$Bu$_3$ArO–H by 18.4 (gas phase) and 19.8 (toluene SCRF) kcal mol$^{-1}$. This supports the experimental conclusion and indicates that **4** is a kinetic rather than thermodynamic product of the reaction.

Solutions of **1** containing the radical trap 1,1-diphenylethylene[22] are stable for days. This suggests that loss of the trifluoroethoxyl radical CF$_3$CH$_2$O$^\bullet$ is not occurring.

Surprisingly, the analogous reaction of **2** with 1 equiv of $^t$Bu$_3$ArO$^\bullet$ under identical conditions (toluene-$d_8$ or DCM-$d_2$/1% MeCN-$d_3$ (v/v)) results in no reaction after 12 h (eq 7). This is an important result, as it shows that oxidation of the alkoxide is not facile.

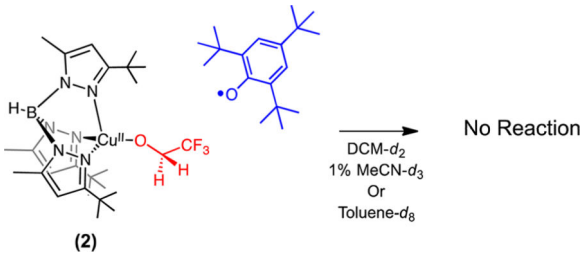


(7)

## Reactions with 2,2,6,6-Tetramethylpiperidine-*N*-oxyl

Treatment of **1** with 1 equiv of TEMPO in DCM-$d_2$/1% MeCN-$d_3$ (v/v) resulted in a color change from red-orange to pale pink after 3 h. The $^1$H and $^{19}$F NMR spectra showed Tp$^{t\text{Bu}}$Cu$^{I}$-MeCN-$d_3$ as well as 0.5 equiv of CF$_3$CH$_2$OH and 0.25 equiv of 2,2,2-trifluoroethyl trifluoroacetate[23] (eq 8). The absence of TEMPO-derived $^1$H NMR resonances and the pinkish hue of the completed reaction mixture suggested that TEMPO was not consumed during the reaction. However, quantification of remaining TEMPO was not

performed. The same organic products were observed when the reaction was performed in toluene-$d_8$.

$$\mathrm{Tp^{tBu}Cu^{II}{-}OCH_2CF_3{+}TEMPO{+}MeCN{-}}d_3 \rightarrow \mathrm{Tp^{tBu}Cu^{I}{-}MeCN{-}}d_3{+}1/2\mathrm{HOCH_2CF_3} + 1/4\mathrm{CF_3COOCH_2CF_3} \quad (8)$$

The reaction between **2** and 1 equiv of TEMPO in DCM-$d_2$/1% MeCN-$d_3$ (v/v) yielded $Tp^{tBuMe}Cu^{I}$-MeCN-$d_3$ and the same organic products but required ~6 h to reach completion. Surprisingly, in toluene-$d_8$ solvent no reaction was observed between **2** and TEMPO.

Monitoring the kinetics of **1** or **2** + TEMPO showed complex behavior. With **1** the reaction began immediately upon addition of TEMPO, and the disappearance of **1** appeared to be zero order. With **2**, there was a 3 h induction period followed by a similar zero-order reaction. When a second equivalent of **2** was added to the completed reaction mixture, it was consumed in the same fashion but with no induction period (Figure 4). This type of behavior is suggestive of an autocatalytic process.[24]

## DISCUSSION

### Cu(II) Alkoxides as H Atom Abstractors

While the literature has discussed $Cu^{II}$-alkoxides as easily oxidized and as H atom donors, $Tp^{tBu}Cu^{II}$–$OCH_2CF_3$ **1** and $Tp^{tBuMe}Cu^{II}$–$OCH_2CF_3$ **2** act as oxidants in their ability to abstract H atoms from substrates (Scheme 4). This is only an inner-sphere oxidizing power, with reduction of copper coupled to formation of an O–H bond. Outer-sphere reduction appears to be less favorable based on the negative electrochemical peak potentials ($E_{p,c}$ ca. − 0.9 V vs $Fc^{+/0}$, though these may be affected by slow electron transfer kinetics). Formation of Cu(I) complexes with hard alkoxide ligands is likely disfavored, but this is ameliorated in the inner-sphere process by protonation of the alkoxide. The ability of a complex to abstract $H^{\bullet}$ is related not only to its reduction potential but also to the basicity of the reduced form.[16] Formation of Cu(I) products in this system is also likely favored by bulky Tp ligands that enforce trigonal pyramidal structures that stabilize Cu(I) over Cu(II). The instability of the trifluoroisopropoxide **3** and the nonfluorinated $Tp^{tBu}$CuOEt is probably a result of the oxidizing nature of these compounds and the increased ease of oxidation of these ligands.

The reactions of **1** and **2** with X–H species overall involve transfer of the proton to the alkoxide ligand and transfer of the electron to Cu(II). Mechanistically, there are five reasonable pathways: (i) sequential electron transfer/proton transfer (ET/PT), (ii) sequential proton transfer/electron transfer (PT/ET), (iii) protolytic ligand exchange followed by radical dissociation, (iv) sequential radical dissociation/HAT, or (v) concerted proton–electron transfer (CPET)[25] equivalent to HAT.

Sequential ET/PT and PT/ET mechanisms (mechanisms (i) and (ii)) are very unlikely because of the high thermodynamic barrier for either initial electron transfer or initial proton

transfer. Both **1** and **2** are very poor outer-sphere oxidants from their irreversible cathodic peak potentials ($E_{p,c} \leq -0.86$ V in DCM vs $Fc^{+/0}$). The H atom donors used here are very poor one-electron reductants ($E°(^{t}Bu_3ArO–H) = +1.18$ V,[16] $E°$(TEMPO–H) = +0.71 V,[16] $E_{p,a}(^{t}Bu_2NPArO–H) = +0.975$ V[19] in MeCN vs $Fc^{+/0}$). Even though the potentials are in different solvents, it is clear that an initial electron transfer step is thermodynamically unfavorable in these systems. Likewise, neither **1** or **2** are especially strong bases, not protonated by [DBU-$H^+$][$^-$OTf] ($pK_a = 24$ [all $pK_a$ values in MeCN]),[14] and **1** is only partially protonated by [Lut-$H^+$][$^-$OTf] ($pK_a = 14.1$).[14] Since the X–H reagents are poor acids ($pK_a(^{t}Bu_3ArO–H) = 28$,[16] $pK_a$(TEMPO–H) = 41,[16] $pK_a(^{t}Bu_2NPArO–H) = 24$[19]), initial proton transfer is an unlikely path.

Initial dissociation of the trifluoroethoxyl radical (mechanism (iii)) seems unlikely based on the absence of reactivity observed between **1** and the radical trap 1,1-diphenylethylene.[22]

Net HAT from XO–H to $Tp^{tBuR}Cu^{II}–OR_f$ could also occur via initial protolytic ligand exchange to give $R_fO–H$ and $Tp^{tBuR}Cu^{II}$-X, followed by rapid dissociation of $X^•$ (mechanism (iv)). However, this mechanism is not accessible for the oxidation of 1,4-cyclohexadiene (eq 3). In addition, the reaction is fastest with TEMPO–H that has the weakest OH bond and slows with increasing OH BDFE (Scheme 4). This correlation of reaction rate with BDFE is predicted by the Marcus model for CPET.[26] The slower reaction of **1** with 1,4-cyclohexadiene is also consistent with a CPET pathway, since C–H bonds are known to react much slower than O–H bonds of the same strength.[26] Thus, the data are most consistent with a direct CPET (HAT) mechanism for the oxidations by **1** and **2**.

## Thermodynamic Implications: Assessment of Effective Bond Dissociation Free Energies

The quantitative reactions of **1** and **2** with H atom donors provide thermochemical information about the copper complexes, including some insights into the unusual H atom transfer reactivity and lack thereof. Summing the net HAT reaction for **1** + $^{t}Bu_3ArOH$ in toluene (eq 9) with the X–H BDFE (eq 10)[16] yields eq 11 that defines an *effective* BDFE for $1/2[Tp^{tBu}Cu^{I}]_2 + HOCH_2CF_3$.[27]

$$\mathbf{1} + {}^{t}\mathrm{Bu_3ArO-H} \rightarrow 1/2[\mathrm{Tp}^{t\mathrm{Bu}}\mathrm{Cu}^{\mathrm{I}}]_2 + \mathrm{HOCH_2CF_3} + {}^{t}\mathrm{Bu_3ArO}^{\bullet}$$

$$\Delta G^{\circ} \leq 0 \text{ kcal mol}^{-1} \quad (9)$$

$${}^{t}\mathrm{Bu_3ArO}^{\bullet} + {}^{\bullet}\mathrm{H} \rightarrow {}^{t}\mathrm{Bu_3ArO-H}$$

$$\Delta G^{\circ} = -76.7 \pm 0.5 \text{ kcal mol}^{-1} \quad (10)$$

$$\mathrm{Tp^{tBu}Cu^{II}-OCH_2CF_3 + {}^{\bullet}H \rightarrow 1/2[Tp^{tBu}Cu^{I}]_2 + HOCH_2CF_3}$$

$$\Delta G^{\circ} \leq -77 \text{ kcal mol}^{-1}$$

$$\mathrm{BDFE\{1/2[Tp^{tBu}Cu^{I}]_2 + HOCH_2CF_3\}} \geq 77 \text{ kcal mol}^{-1} \quad (11)$$

An analogous assessment for **2** using its reaction with ABNO–H gives an effective BDFE of ≥71 kcal $mol^{-1}$.

It must be emphasized that these effective BDFE values are not solely bond cleavage reactions. Reaction 11 includes (i) transfer a hydrogen atom to $Tp^{tBuR}Cu^{II}OCH_2CF_3$, (ii) dissociation of $HOCH_2CF_3$ from $Tp^{tBuR}Cu^{I}$, and (iii) dimerization to $1/2[Tp^{tBuR}Cu^{I}]_2$. It has been reported by Tolman[7c] and Parkin[8b] that $[Tp^{tBu}Cu^{I}]_2$ and $[Tp^{tBuMe}Cu^{I}]_2$ dimers are stable to dissociation even at 90 °C in the absence of a Lewis base, so the thermochemical contribution from their formations in these reactions is likely not negligible. Similar estimates can be derived from the reactions in DCM/MeCN, where the Cu(I) product is stabilized by binding MeCN to form $[Tp^{tBuR}Cu^{I}(MeCN)]$.

The effective BDFEs can be combined with the gas-phase thermochemistry of dehydrogenation of $CF_3CH_2OH$ to give insight into the net thermodynamics associated with oxidation of the alkoxide ligand via HAT/ET and formation of $1/2[Tp^{tBuR}Cu^{I}]_2$. Equivalently, this analysis gives the composite “effective α-C–H BDFE” of the alkoxide ligand.

$$\mathrm{Tp^{tBu}Cu^{II}-OCH_2CF_3 + {}^{\bullet}H \rightarrow 1/2[Tp^{tBu}Cu^{I}]_2 + HOCH_2CF_3}$$

$$\Delta G^{\circ} \leq -77 \text{ kcal mol}^{-1} \quad (12)$$

$$\mathrm{H-OCH_2CF_3 \rightarrow O{=}CH(CF_3) + H_2}$$

$$\Delta G^{\circ} = 17.5 \pm 3 \text{ kcal mol}^{-1} \quad (13)$$

$$\mathrm{H_2 \rightarrow 2H^{\bullet}}$$

$$\Delta G^{\circ} = 97.2 \text{ kcal mol}^{-1} \quad (14)$$

The sum of eqs 12, 13,[28] and 14[29] gives eq 15:

$$\mathrm{Tp}^{t\mathrm{Bu}}\mathrm{Cu}^{\mathrm{II}} - \mathrm{OCH_2CF_3} \rightarrow 1/2[\mathrm{Tp}^{t\mathrm{Bu}}\mathrm{Cu}^{\mathrm{I}}]_2 + \mathrm{O{=}CHCF_3} + \mathrm{H}^{\bullet}$$

$$\Delta G^{\circ} \leq 38 \text{ kcal mol}^{-1} \quad (15)$$

The analogous calculation for **2** using its effective BDFE given above gives eq 16:

$$\mathrm{Tp}^{t\mathrm{BuMe}}\mathrm{Cu}^{\mathrm{II}} - \mathrm{OCH_2CF_3} \rightarrow 1/2[\mathrm{Tp}^{t\mathrm{BuMe}}\mathrm{Cu}^{\mathrm{I}}]_2 + \mathrm{O{=}CHCF_3} + \mathrm{H}^{\bullet}$$

$$\Delta G^{\circ} \leq 44 \text{ kcal mol}^{-1} \quad (16)$$

A key point of this exercise is to estimate the free energy of the *unobserved* alkoxide oxidation analogous to Scheme 1 above. The free energy for this reaction for **2** (eq 17) is given by the sum of eq 16 and the $^{t}$Bu$_3$ArO–H BDFE (eq 10). The same value is obtained for the reaction in DCM/MeCN with Tp$^{t\mathrm{BuMe}}$Cu$^{\mathrm{I}}$(MeCN) as a product. The analogous value for the reaction of **1** has a 6 kcal mol$^{-1}$ more negative limit.

$$\mathrm{Tp}^{t\mathrm{BuMe}}\mathrm{Cu}^{\mathrm{II}} - \mathrm{OCH_2CF_3} + {}^{t}\mathrm{Bu_3ArO}^{\bullet} \rightarrow 1/2[\mathrm{Tp}^{t\mathrm{BuMe}}\mathrm{Cu}^{\mathrm{I}}]_2 + \mathrm{O{=}CHCF_3} + {}^{t}\mathrm{Bu_3ArOH}$$

$$\Delta G^{\circ} \leq -33 \text{ kcal mol}^{-1} \quad (17)$$

Reaction 17 is very exoergic. This conclusion seems solid despite the approximations used, such as the mixing of solution and gas-phase free energies. In this light, the observation that $^{t}$Bu$_3$ArO$^{\bullet}$ does not react with **2** must be the result of a high barrier along the path to Cu(I) products associated with one of the elementary steps comprising the net reaction depicted in eq 16.

## Possible Origin for the Unreactive Nature of 2 with $^{t}$Bu$_3$ArO$^{\bullet}$

The consensus mechanism of alkoxide oxidation in galactose oxidase is that the rate-determining step involves hydrogen atom transfer from the alkoxide α-C–H to a tyrosyl radical. There is some evidence that this process may occur concertedly with electron transfer to Cu(II),[1i] although it is generally thought that the transition state is dominated by hydrogen atom transfer with only minor contributions from electron transfer event.[1f] This HAT/ET step is apparently not facile for **2** + $^{t}$Bu$_3$ArO$^{\bullet}$. If this step were facile, it would form

the $Tp^{tBuMe}Cu^{I}(O{=}CHCF_3)$ adduct, which would likely undergo very facile solvolysis in DMC/MeCN to $Tp^{tBuMe}Cu^{I}(MeCN)$ (Scheme 5).

From a thermodynamics standpoint, the HAT/ET step requires that the copper center weaken the α-C–H bond of the alkoxide. In the enzymatic reaction, the α-C–H bond of the primary alcohol is ca. 8 kcal $mol^{-1}$ stronger than the tyrosine O–H bond formed.[3] This has been explained by citing the weakening in α-C–H bond strengths of alcohols upon deprotonation[30] or formation of strong hydrogen bonds.[31] Theoretical studies have shown this effect can be quite substantial as methanol deprotonation results in α-C–H bond weakening of ca. 10 and 12 kcal $mol^{-1}$ for $NaOCH_3$ and $KOCH_3$, respectively.[30b] This is due to the formation of a three-electron two-center bond between the radical and the high-energy alkoxide lone pair in the left resonance structure in Scheme 6.

Such α-C–H bond weakening should occur in copper(II) alkoxide complexes. However, this effect seems insufficient in this case to allow HAT/ET to occur between **2** and $^{t}Bu_3ArO^{\bullet}$. ENDOR studies have shown the copper–oxygen bond in **1** (considered roughly analogous to **2**) is relatively ionic, although ~15% radical character is centered on oxygen.[11] The calculated α-C–H bond dissociation enthalpy (BDE) in trifluoroethanol is 97 kcal $mol^{-1}$, while the BDE of the O–H bond that would be formed in $^{t}Bu_3ArO$–H is ~82 kcal $mol^{-1}$.[3,32] Thus, an ~15 kcal $mol^{-1}$ weakening would be required for the HAT/ET step in Scheme 5 to be thermoneutral. This is larger than the ca. 8 kcal $mol^{-1}$ given above for the enzymatic reaction, both because $^{t}Bu_3ArO^{\bullet}$ is a weaker abstractor than tyrosyl and because the α-C–H bond is stronger in trifluoroethanol than a simple primary alcohol.[3,30c,32] In addition to this thermochemical difficulty with the HAT/ET step, there may also be a kinetic barrier due to a polar effect on HAT due to the electron-withdrawing CF3 group[26] and/or steric crowding in the system. However, it seems unlikely that steric crowding would be the only limiting factor, since **2** reacts with hydrogen atom donors with equal steric profiles under the same conditions.

## CONCLUSIONS

Model complexes (**1**) ($Tp^{tBu}Cu^{II}$–$OCH_2CF_3$) and (**2**) ($Tp^{tBuMe}Cu^{II}$–$OCH_2CF_3$) were prepared as models for the reactive intermediates involved in Cu/radical alcohol oxidation catalysts. These complexes are reasonably strong hydrogen atom *acceptors* capable of cleaving the O–H bonds with BDFEs up to 77 and 71 kcal $mol^{-1}$, respectively. On the basis of thermodynamics and kinetics arguments, we conclude these reactions proceed through concerted proton–electron transfer mechanisms (CPET).

The strongly oxidizing nature of **1** and **2** makes the oxidation of their coordinated alkoxide ligands by the tri-*t*-butylphenoxyl radical quite favorable. An overall $\Delta G^{\circ} < -33$ kcal $mol^{-1}$ to form Cu(I) complexes and $O{=}CHCF_3$ is estimated from thermochemical cycles. Yet no reaction is observed between **2** and $^{t}Bu_3ArO^{\bullet}$, and **1** undergoes an alternative unusual alkoxyl radical transfer reaction. Because **2** is unreactive with $^{t}Bu_3ArO^{\bullet}$ we suggest the α-C–H bond in the trifluoroethoxide ligand is not sufficiently weakened compared to the free alcohol to facilitate hydrogen atom transfer. This system, examining rare examples of

Cu(II)-alkoxide complexes, thus provides insights into the copper/radical mediated alcohol oxidation reactions in both biological and synthetic organic chemistry.

## EXPERIMENTAL SECTION

### General Considerations

Unless otherwise noted, all reactions were preformed in a nitrogen-filled glovebox at ambient temperatures. Compounds (**1**), (**2**), and (**3**) were found to be very sensitive to trace contaminants so all glassware was washed with aqua regia (3:1 $HCl/HNO_3$) and rinsed thoroughly prior to being dried at 150 °C overnight and pumped into a nitrogen-filled glovebox. Compounds (**1**), (**2**), and (**3**) were found to be mildly light-sensitive, so they were stored in the dark at −30 °C. All NMR reactions were performed in NMR tubes protected from light with aluminum foil. ***Caution!*** *Aqua regia is highly corrosive and extremely dangerous. Special care should be taken when using it.*

### Materials

Unless otherwise noted, all chemicals were purchased from Sigma-Aldrich and used without purification. Dichloromethane-$d_2$, acetonitrile-$d_3$, toluene-$d_8$, and 2,2,2-trifuoroethanol-$d_3$ were purchased from Cambridge Isotope Laboratories. Dichloromethane-$d_2$ and acetonitrile-$d_3$ were dried over $CaH_2$, and toluene-$d_8$ was dried over NaK [***Caution!*** *Pyrophoric*] and vacuum-distilled. 2,2,2-trifluoroethanol and 1,1,1-trifluoro-2-propanol were distilled from $CaSO_4$ with a small amount of $NaHCO_3$ and stored over 3 Å molecular sieves. Acetonitrile was used as received from Burdick and Jackson (low water) and was stored in an argon-pressurized stainless steel drum, plumbed directly into a glovebox.

Other solvents were purchased from Fischer and dried using a “Grubbs-type” Seca Solvent System installed by GlassContour. TEMPO was purified by sublimation. TEMPO–H,[33] $^t$Bu$^3$ArO$^\bullet$,[18] $^t$Bu$_2$NPArO–H,[19] $^t$Bu$_2$NPArO$^\bullet$,[19] [DBUH$^+$][OTf$^-$],[34] [LutH$^+$]-[OTF$^-$],[35] Tp$^{t\mathrm{Bu}}$Cu$^{\mathrm{II}}$–Cl,[7d] [Tp$^{t\mathrm{Bu}}$Cu$^{\mathrm{I}}$]$_2$,[7c] Tp$^{t\mathrm{Bu}}$Cu$^{\mathrm{I}}$-MeCN,[7c] Tp$^{t\mathrm{BuMe}}$Cu$^{\mathrm{II}}$–Cl,[8b] [Tp$^{t\mathrm{BuMe}}$Cu$^{\mathrm{I}}$]$_2$,[8b] and Tp$^{t\mathrm{BuMe}}$Cu$^{\mathrm{I}}$-MeCN[36] were prepared using established literature protocols. All glassware was dried in an oven at 150 °C overnight and pumped into a nitrogen-filled glovebox while hot. Celite was dried at 100 °C overnight under vacuum.

### Instrumentation

All $^1$H (and $^{19}$F) NMR spectra were obtained on Bruker 300 (282) and 500 (470) MHz instruments. The $^1$H chemical shifts reported are referenced to tetramethylsilane using the residual solvent peak, and $^{19}$F chemical shifts are referenced to a fluorobenzene internal standard. UV–visible absorption spectra were collected with a Hewlett-Packard 8453 diode array spectrometer equipped with a Unisoku USP-203 cryostat. EPR spectra were collected on a Bruker EMX CW X-band spectrometer. Cyclic voltammetry was performed using a CH Instruments 600D potentiostat. CHN elemental analysis was performed by Atlantic Microlabs, Inc, Norcross, GA.

### Representative Reaction Screening Procedure

In a nitrogen-filled glovebox, a $^{t}Bu_3ArOH$ solution (300 μL, 30.6 mM DCM-$d_2$/1% MeCN-$d_3$ (v/v)) was added dropwise to a solution of $Tp^{tBu}Cu^{II}–OCH_2CF_3$ (300 μL, 30.6 mM DCM-$d_2$/1% MeCN-$d_3$ (v/v)) with stirring. The resulting solution was transferred to a J. Young tube stored at room temperature in the dark until the reaction had reached completion.

### Syntheses. Hydro-tris(3-tert-butylpyrazol-1-yl)borate) Cu(II) triflate, $Tp^{tBu}Cu^{II}–OTf$

$Tp^{tBu}Cu^{II}–OTf$ was prepared as previously described with minor modifications.[7a] To a 5 mL toluene solution of $Tp^{tBu}Cu^{II}–Cl$ (495 mg, 1.03 mmol) was added a 3 mL solution of AgOTf (264 mg, 1.03 mmol) with stirring. The reaction mixture rapidly changed colors from brown to deep purple, and a thick precipitate of AgCl and $Tp^{tBu}Cu^{II}–OTf$ was formed. The solid mixture was collected by filtration, washed with toluene (3 × 5 mL), and dried under vacuum. Extraction with DCM followed by filtration over Celite gave a deep purple solution, which upon removal of the solvent, yielded $Tp^{tBu}Cu^{II}–OTf$ as a black solid (569 mg, 93% yield). $^1$H NMR (500 MHz, $CD_2Cl_2$) δ: 56.51 (broad, 3H), 20.98 (broad, 3H), 5.54 (broad, 27H), −5.38 (broad, 1H).

### Hydro-tris(3-tert-butyl-5-methyl-pyrazol-1-yl)borate) Cu(II), $Tp^{tBuMe}Cu^{II}–OTf$

To a 5 mL toluene solution of $Tp^{tBuMe}Cu^{II}–Cl$ (354 mg, 0.68 mmol) was added a 3 mL solution of AgOTf (175 mg, 0.68 mmol) with stirring. The reaction mixture rapidly changed colors from brown to deep purple. After 10 min, the resulting solution was filtered over Celite, and the solvent was removed in vacuo to yield $Tp^{tBuMe}Cu^{II}–OTf$ as a black solid (411 mg, 95%). $^1$H NMR (500 MHz, $CD_2Cl_2$) δ: 59.0 (broad, 3H), 10.42 (broad, 9H), 4.51 (broad, 27H), −5.97 (broad, 1H).

### Hydro-tris(3-tert-butylpyrazol-1-yl)borate) Cu(II) 2,2,2-trifluoroethoxide, $Tp^{tBu}Cu_{II}–OCH_2CF_3$ (1)

A 2 mL DCM solution containing DBU (39.1 mg, 0.26 mmol) and 2,2,2-trifluoroethanol (77.0 mg, 0.79 mmol) was added dropwise to a 15 mL stirring DCM solution of $Tp^{tBu}Cu^{II}–OTf$ (152 mg, 0.26 mmol), upon which the reaction solution changed colors from deep purple to orange. After 10 min the solvent was removed in vacuo, and the remaining solid was redissolved in a minimum amount of pentane and filtered. Large orange X-ray quality crystals grew upon standing at −30 °C (49.4 mg, 35%). $^1$H NMR (500 MHz, $CD_2Cl_2$) δ: 40.55 (broad, 3H), 18.42 (broad, 3H), 4.36 (broad, 27H), −5.37 (broad, 1H). $^{19}$F (470 MHz, $CD_2Cl_2$) δ: −65.9 (broad, 3F) UV/vis: $\lambda_{max}$ = 424 nm (3500 ± 350 $M^{-1}$ $cm^{-1}$), 886 nm (160 ± 20 $M^{-1}$ $cm^{-1}$). Anal. Calcd for $C_{23}H_{36}BCuF_3N_6O$: C, 50.79; H, 6.67; N, 15.45. Found: C, 51.03; H, 6.56; N, 15.65%.

### Hydro-tris(3-tert-butylpyrazol-1-yl)borate) Cu(II) 2,2,2-trifluoroethoxide-$d_2$, $Tp^{tBu}Cu^{II}–OCD_2CF_3$

$Tp^{tBu}Cu^{II}–OCD_2CF_3$ was prepared in the same manner as (**1**), but 2,2,2-trifluoroethanol-$d_3$ was used in place of proteo-2,2,2-trifluoroethanol.

### Hydro-tris(3-tert-butyl-5-methyl-pyrazol-1-yl)borate) Cu(II) 2,2,2-trifluoroethoxide, $Tp^{tBuMe}Cu^{II}–OCH_2CF_3$ (2)

$Tp^{tBuMe}Cu^{II}–OCH_2CF_3$ was prepared in the same manner as described for $Tp^{tBu}Cu^{II}–OCH_2CF_3$ (14% yield). $^1H$ NMR (500 MHz, $CD_2Cl_2$) δ: 43.3 (3H), 4.28 (27H), 1.98 (9H), –5.85 (1H). $^{19}F$ (470 MHz, $CD_2Cl_2$) δ: −66.52. UV/vis: $\lambda_{max}$ = 423 nm (3300 ± 330 $M^{-1}$ $cm^{-1}$), 902 nm (130 ± 20 $M^{-1}$ $cm^{-1}$). Anal. Calcd for $C_{26}H_{42}BCuF_3N_6O$: C, 53.29; H, 7.22; N, 14.34. Found: C, 53.34; H, 7.38; N, 14.34%.

### Hydro-tris(3-tert-butylpyrazol-1-yl)borate) Cu(II) 1,1,1-trifluoro-2-propoxide, $Tp^{tBu}Cu^{II}–OCH(CH_3)CF_3$ (3)

$Tp^{tBuMe}Cu^{II}–OCH(CH_3)$-$CF_3$ was prepared in the same manner as described for $Tp^{tBu}Cu^{II}–OCH_2CF_3$ (61% yield). $^1H$ NMR (500 MHz, $CD_2Cl_2$) δ: 39.60 (broad, 3H), 19.34 (broad, 3H), 4.30 (27H), −4.59 (1H). $^{19}F$ (470 MHz, $CD_2Cl_2$) δ: −65.52 (3H, broad). UV/vis: $\lambda_{max}$ = 432 nm (3900 ± 390 $M^{-1}$ $cm^{-1}$), 869 nm (130 ± 20 $M^{-1}$ $cm^{-1}$). Anal. Calcd for $C_{24}H_{38}BCuF_3N_6O$: C, 51.66; H, 6.87; N, 15.06. Found: C, 51.72; H, 6.77; N, 15.27%.

### Azabicyclo[3.3.1]nonane N-hydroxide, ABNO–H

In an argon-filled “wet box”, $Na_2S_2O_4$ (300 mg, 1.72 mmol) in ~3 mL of water was added to an ~5 mL 1:1 acetone/water solution of ABNO (150 mg, 1.07 mmol) with stirring. After 30 min, acetone was removed under vacuum leaving water and an insoluble white precipitate. The white precipitate was extracted with pentane (3 × 5 mL) and filtered. Pentane was removed under vacuum leaving a white solid. Repeated dissolution in ether and removal of solvent under vacuum served to remove residual water remaining from the reaction (122 mg; 81% yield). The $^1H$ NMR spectrum was consistent with ABNO–H prepared via a different synthetic route previously reported.[37]

## Supplementary Material

Refer to Web version on PubMed Central for supplementary material.

## Acknowledgments

The authors thank Prof. S. Stoll and E. Hayes with assistance with EPR measurements and simulations and Prof. R. Knowles for useful discussions about α-C–H bond strengths of alkoxides. We gratefully acknowledge financial support from the U.S. National Institute of Health (2R01GM50422).

## REFERENCES

1. (a) Branchaud BP, Montague-Smith MP, Kosman DJ, McLaren FR. J. Am. Chem. Soc. 1993; 115:798.(b) Wachter RM, Branchaud BP. J. Am. Chem. Soc. 1996; 118:2782.(c) Wachter RM, Montague-Smith MP, Branchaud BP. J. Am. Chem. Soc. 1997; 119:7743.(d) Turner BE, Branchaud BP. Bioorg. Med. Chem. Lett. 1999; 9:3341. [PubMed: 10612596] (e) Jazdzewski BA, Tolman WB. Coord. Chem. Rev. 2000; 200–202:633.(f) Himo, Fahmi, Eriksson LA, Maseras F, Siegbahn PEM. J. Am. Chem. Soc. 2000; 122:8031.(g) Whittaker MM, Whittaker JW. Biochemistry. 2001; 40:7140. [PubMed: 11401560] (h) Branchaud BP, Turner BE. Methods Enzymol. 2002; 354:415. [PubMed: 12418243] (i) Whittaker JW. Chem. Rev. 2003; 103:2347. [PubMed: 12797833] (j) Whittaker JW. Arch. Biochem. Biophys. 2005; 433:227. [PubMed: 15581579] (k) Pratt RC, Stack TDP. Inorg. Chem. 2005; 44:2367. [PubMed: 15792472] (l) Lyons CT, Stack DP. Coord. Chem. Rev. 2013; 257:528. [PubMed: 23264696]

2. (a) Sheldon RA, Arends IWCE. Adv. Synth. Catal. 2004; 346:1051.(b) Hoover JM, Ryland BL, Stahl SS. J. Am. Chem. Soc. 2013; 135:2357. [PubMed: 23317450] (c) Hoover JM, Ryland BL, Stahl SS. ACS Catal. 2013; 3:2599. [PubMed: 24558634] (d) Cao Q, Dornan LM, Rogan L, Hughes NL, Muldoon ML. Chem. Commun. 2014; 50:4524.(e) Ryland BL, McCann SD, Brunold TC, Stahl SS. J. Am. Chem. Soc. 2014; 136:12166. [PubMed: 25090238] (f) Ryland BL, Stahl SS. Angew. Chem. Int. Ed. 2014; 53:8824.
3. Luo, Y-R. Comprehensive Handbook of Chemical Bond Energies. Boca Raton, FL: CRC Press; 2007.
4. Gephart RT III, McMullin CL, Sapiezynski NG, Jang ES, Aguila MJR, Cundari TR, Warren TH. J. Am. Chem. Soc. 2012; 134:17350. [PubMed: 23009158]
5. (a) Jeffries PM, Wilson SR, Girolami GS. Inorg. Chem. 1992; 31:4503.(b) Goel SC, Kramer KS, Chiang MY, Buhro WE. Polyhedron. 1990; 9:611.(c) Chi Y, Hsu PF, Liu CS, Ching WL, Chou TY, Carty AJ, Peng SM, Lee GH, Chuang SH. J. Mater. Chem. 2002; 12:3541.
6. Tubbs KJ, Fuller AL, Bennett B, Arif AM, Berreau LM. Inorg. Chem. 2003; 42:4790. [PubMed: 12895095]
7. (a) Tolman WB. Inorg. Chem. 1991; 30:4877.(b) Carrier SM, Ruggiero CE, Tolman WB. J. Am. Chem. Soc. 1992; 114:4407.(c) Carrier SM, Ruggiero CE, Houser RP, Tolman WB. Inorg. Chem. 1993; 32:4889.(d) Ruggiero CE, Carrier SM, Antholine WE, Whittaker JM, Cramer CJ, Tolman WB. J. Am. Chem. Soc. 1993; 115:11285.
8. (a) Han R, Looney A, McNeill K, Parkin G, Rheingold AL, Haggerty BS. J. Inorg. Biochem. 1993; 49:105.(b) Yoon K, Parkin G. Polyhedron. 1995; 14:811.
9. (a) Kitajima N, Fujisawa K, Tanaka M, Moro-oka T. J. Am. Chem. Soc. 1992; 114:9232.(b) Kitajima N, Katayama T, Fujisawa K, Iwata Y, Moro-oka Y. J. Am. Chem. Soc. 1993; 115:7872.(c) Fujisawa K, Iwata Y, Kitajima N, Higashimura H, Kubota M, Miyashita Y, Yamada Y, Okamoto K, Moro-oka Y. Chem. Lett. 1999; 28:739.(d) Qiu D, Kilpatrick L, Kitajima N, Spiro TG. J. Am. Chem. Soc. 1994; 116:2585.(e) Fujisawa K, Kobayashi T, Fujita K, Kitajima N, Moro-oka Y, Miyashita Y, Yamada Y, Okamoto K. Bull. Chem. Soc. Jpn. 2000; 73:1797.(f) Chen P, Fujisawa K, Solomon EI. J. Am. Chem. Soc. 2000; 122:10177.
10. Trofimenko S, Calabrese JC, Thompson JS. Inorg. Chem. 1987; 26:1507.
11. Hayes EC, Porter TR, Barrows CJ, Kaminsky W, Mayer JM, Stoll S. J. Am. Chem. Soc. 2016; 138:4132.
12. (a) $\tau = [\sum(L_{basal}{-}M{-}L_{basal}) - \sum(L_{basal}{-}M{-}L_{axial})]/90$. Vela J, Stoian S, Flaschenriem CJ, Münck E, Holland PL. J. Am. Chem. Soc. 2004; 126:4522. [PubMed: 15070362]
13. Holm RH, Kennepohl P, Solomon EI. Chem. Rev. 1996; 96:2239. [PubMed: 11848828]
14. Kaljurand I, Kütt A, Sooväli L, Rodima T, Mäemets V, Leito I, Koppel IA. J. Org. Chem. 2005; 70:1019. [PubMed: 15675863]
15. The addition of a small amount of MeCN-$d_3$ to a solution of $Tp^{tBu}Cu^{II}$-OTf in DCM-$d_2$ results in a dramatic change by $^1$H NMR. We attribute this to the formation of [$Tp^{tBu}Cu^{II}$-MeCN-$d_3^+$] [$^-$OTf], although this species was not characterized exhaustively. See Supporting Information for additional details.
16. Warren JJ, Tronic TT, Mayer JM. Chem. Rev. 2010; 110:6961. [PubMed: 20925411]
17. (a) Bond dissociation enthalpies (BDEs) were taken from ref 3 or from ref 16 and converted to gas-phase or solvent-corrected bond dissociation free energies (BDFEs; see refs 16, 17b, and c). These calculations are shown explicitly in the Supporting Information. Litwinienko G, Ingold KU. Acc. Chem. Res. 2007; 40:222. [PubMed: 17370994] Warren JJ, Mayer JM. Proc. Natl. Acad. Sci. U. S. A. 2010; 107:5282. [PubMed: 20215463]
18. Manner VW, Markle TF, Freudenthal JH, Roth JP, Mayer JM. Chem. Commun. 2008:256.
19. Porter TR, Kaminsky W, Mayer JM. J. Org. Chem. 2014; 79:9451. [PubMed: 25184812]
20. Complex (**2**) reacted quantitatively in DCM-$d_2$/1% MeCN-$d_3$ (v/v) with TEMPO–H, ABNO–H, and $^t$Bu$_3$ArO–H to yield $Tp^{tBuMe}Cu^{I}$-MeCN-$d_3$, $HOCH_2CF_3$, and the corresponding oxyl radical. Reactions with (**2**) in DCM-$d_2$/1% MeCN-$d_3$ (v/v) were not attempted with either $^t$Bu$_2$NPArO–H or 1,4-cyclohexadiene.
21. Zhao Y, Truhlar DG. Acc. Chem. Res. 2008; 41:157. [PubMed: 18186612]
22. Korth HG, Chateauneuf J, Lusztyk J, Ingold KU. J. Org. Chem. 1991; 56:2405.

23. (a) Trifluoroethyl trifluoroacetate was identified by GC/MS and by comparison to an independently prepared sample. Grieco PA, Parker DT. J. Org. Chem. 1988; 53:3325.
24. Frenklach M, Clary D. Ind. Eng. Chem. Fundam. 1983; 22:433.
25. Costentin C, Evans DH, Robert M, Savéant J-M, Singh PS. J. Am. Chem. Soc. 2005; 127:12490. [PubMed: 16144387]
26. (a) Mayer JM. Acc. Chem. Res. 2011; 44:36. [PubMed: 20977224] (b) Mayer JM. J. Phys. Chem. Lett. 2011; 2:1481. [PubMed: 21686056]
27. Waidmann CR, Miller AJM, Ng AC–W, Scheuermann ML, Porter TR, Tronic TT, Mayer JM. Energy Environ. Sci. 2012; 5:7771.
28. The enthalpy of dehydrogenation of trifluoroacetaldehyde was calculated from standard heats of formations of 2,2,2-trifluoroethanol (−211.3 kcal $mol^{-1}$)[25b] and trifluoroacetaldehyde (−185.8 kcal $mol^{-1}$; calcd).[25b] Entropic contributions were estimated from the difference in standard molar entropies of ethanol (67.3 cal $mol^{-1}$ $K^{-1}$)[25c] and acetaldehyde (63.0 cal $mol^{-1}$ $K^{-1}$)[25c] + $H_2$ (31.2 cal $mol^{-1}$ $K^{-1}$)[25c] at 298 K ($\Delta S°$ of ethanol/acetaldehyde assumed to be the same as 2,2,2-trifluoroethanol/trifluoroacetaldehyde). Bartmess JE, Liebman J. Struct. Chem. 2013; 24:2035. CRC Handbook of Chemistry and Physics (95th). 2015Boca Raton, FLCRC Press
29. http://webbook.nist.gov/chemistry/
30. (a) Evans BDA, Baillargeon DJ. Tetrahedron Lett. 1978; 19:3315.(b) Steigerwald ML, Goddard WA III, Evans DA. J. Am. Chem. Soc. 1979; 101:1994.(c) Henry DJ, Parkinson CJ, Mayer PM, Radom L. J. Phys. Chem. A. 2001; 105:6750–6756.
31. (a) Gawlita E, Lantz M, Paneth P, Bell AF, Tonge PJ, Anderson VE. J. Am. Chem. Soc. 2000; 122:11660.(b) Jeffrey JL, Terrett JA, MacMillan DWC. Science. 2015; 349:1532. [PubMed: 26316601]
32. Song K-S, Liu L, Guo Q-X. Tetrahedron. 2004; 60:9909.
33. Mader EA, Davidson ER, Mayer JM. J. Am. Chem. Soc. 2007; 129:5153. [PubMed: 17402735]
34. Thomas AM, Lin B-L, Wasinger EC, Stack TDP. J. Am. Chem. Soc. 2013; 135:18912. [PubMed: 24279864]
35. Fan L, Ozerov OV. Chem. Commun. 2005:4450.
36. Muñoz-Molina JMA, Sameera WMC, Álvarez E, Maseras F, Belderrain TSR, Pérez PJ. Inorg. Chem. 2011; 50:2458. [PubMed: 21319785]
37. Nelsen SF, Kessel CR, Brien DJ. J. Am. Chem. Soc. 1980; 102:702.

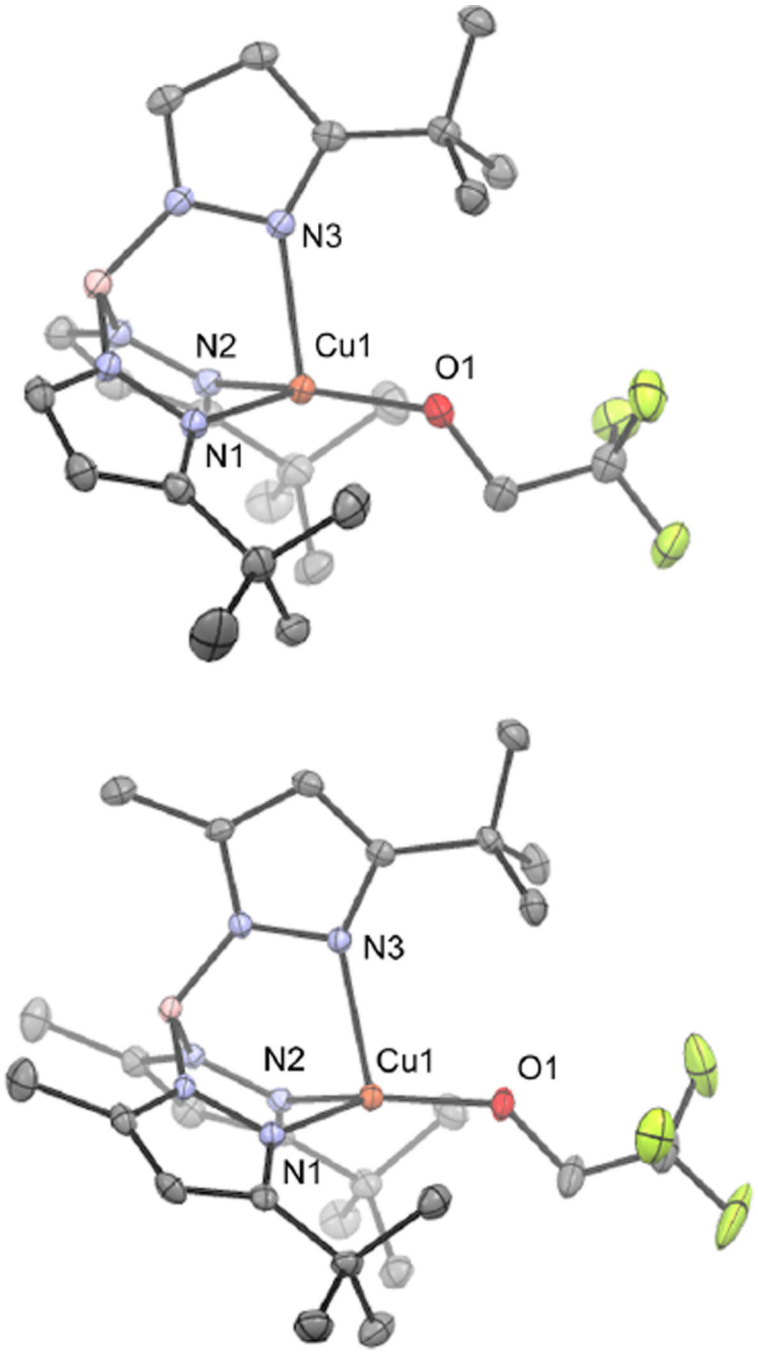


**Figure 1.**
ORTEPs of $Tp^{tBu}Cu^{II}–OCH_2CF_3$ (**1**) (top) and $Tp^{tBuMe}Cu^{II}–OCH_2CF_3$ (**2**) (bottom) showing 50% probability ellipsoids and select atom labels. Hydrogen atoms are omitted for clarity.

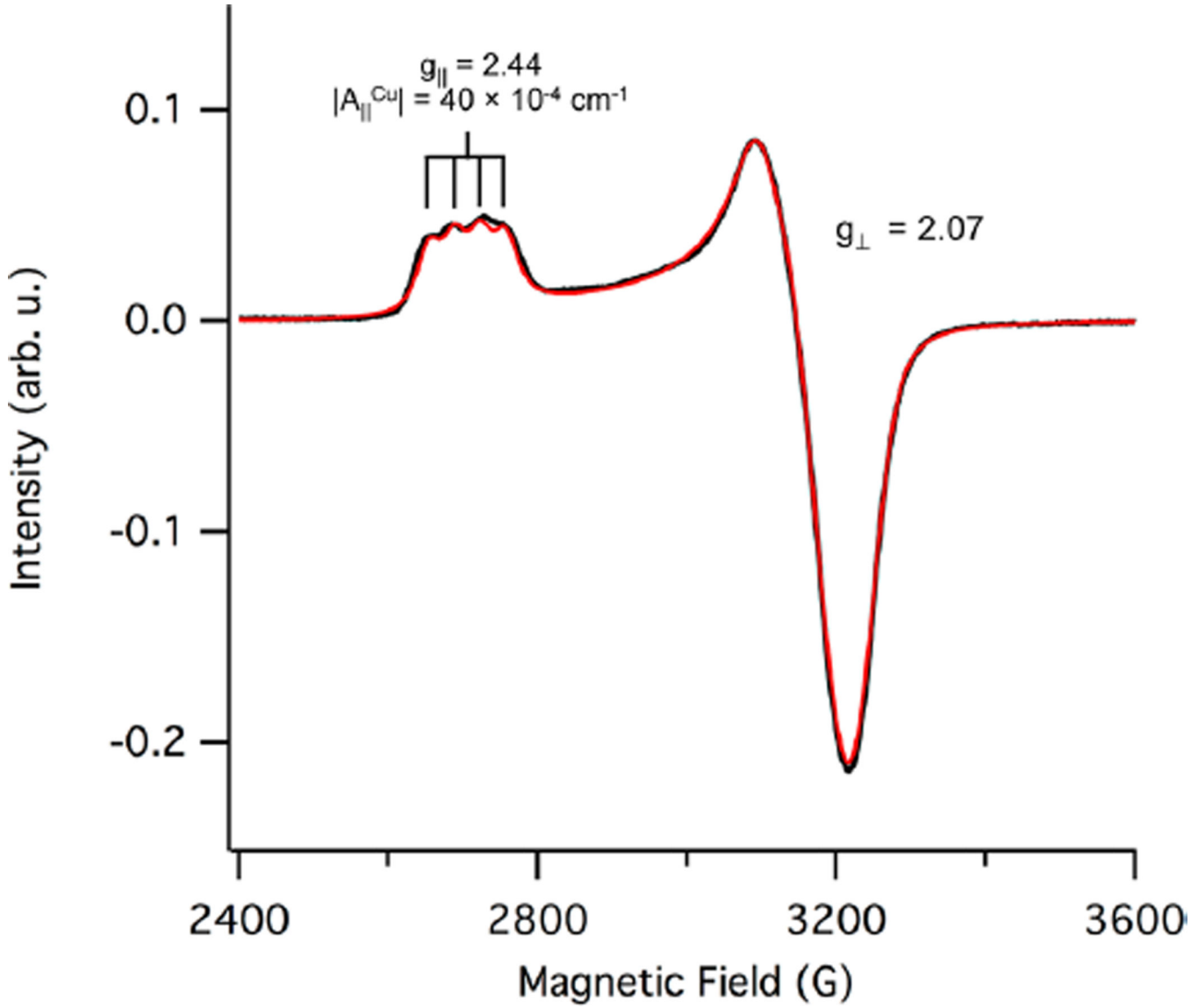


**Figure 2.**

X-band EPR spectrum of **1** in a toluene glass at 120 K. Data are shown in black; simulation is shown in red.

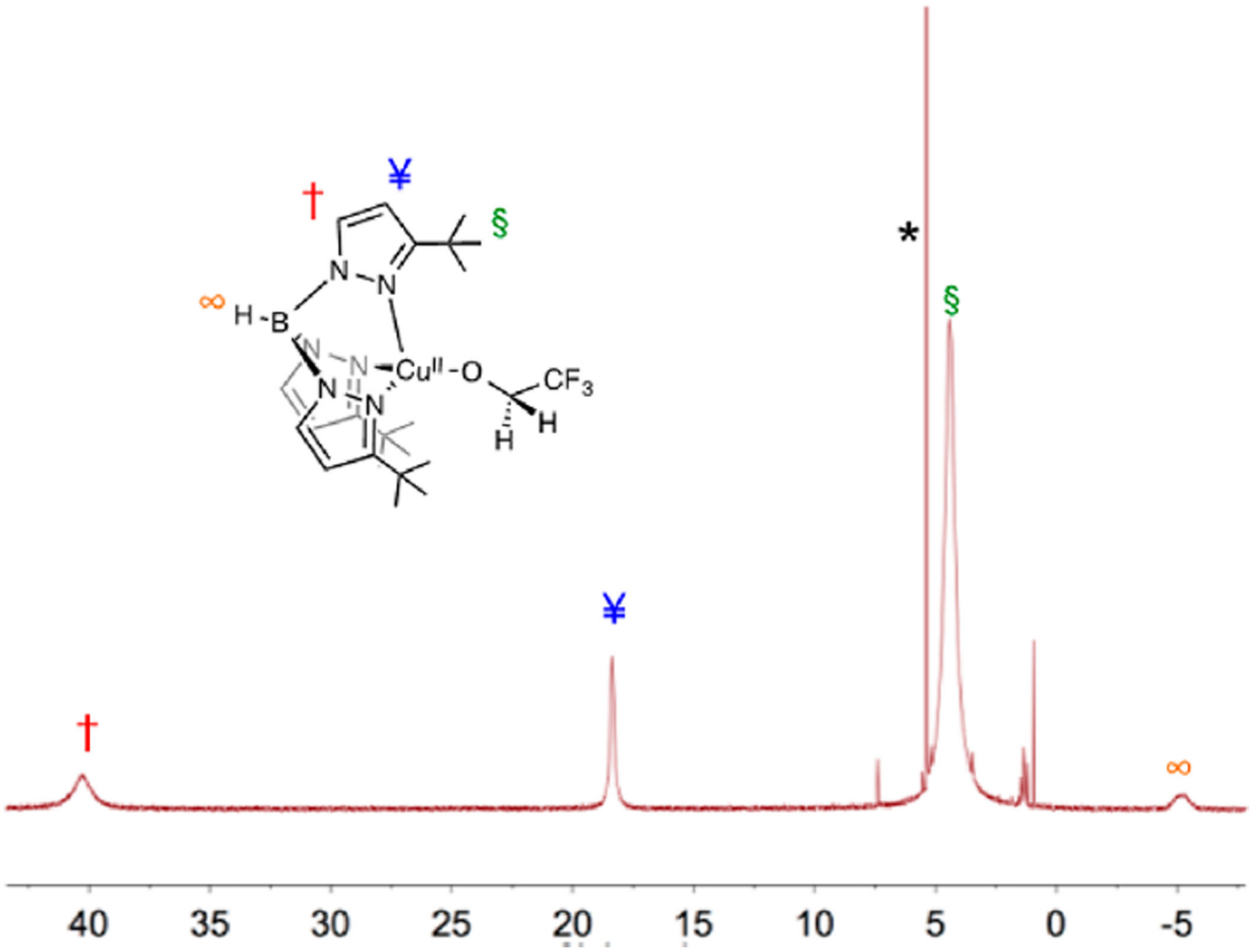


**Figure 3.**

$^1$H NMR spectrum of (**1**) in DCM-$d_2$, with assignments. Residual solvent signal shown with *.

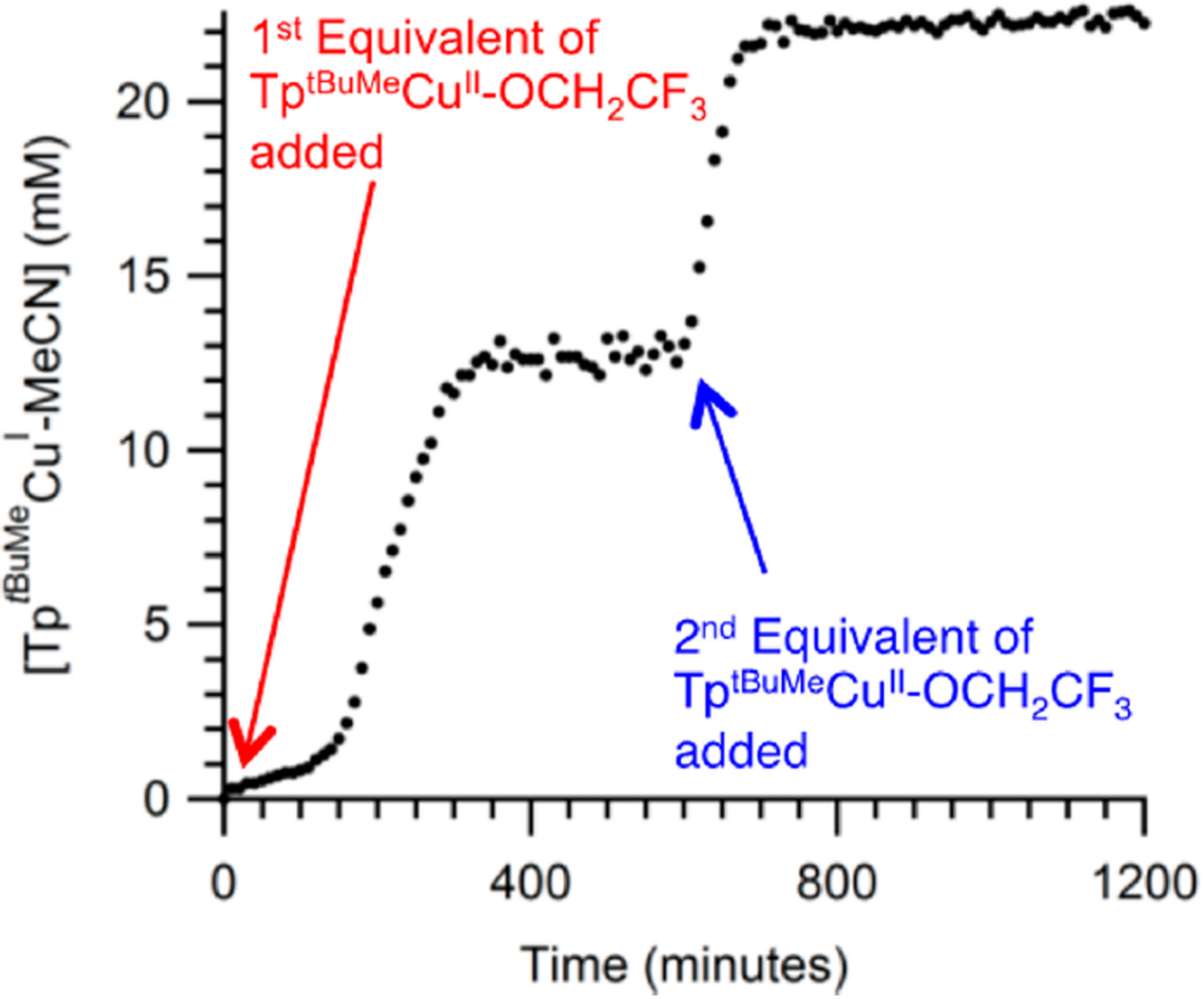


**Figure 4.**

Kinetics trace for the TEMPO-catalyzed disproportionation of $Tp^{tBuMe}Cu^{II}–OCH_2CF_3$ in DCM-$d_2$/1% MeCN-$d_3$ (v/v) to yield $Tp^{tBuMe}Cu^{I}$-MeCN-$d_3$, 0.5 equiv of TFE and 0.25 equiv of trifluoroethyl trifluoroacetate. The time course between 0 and 500 min shows the disproportionation reaction of 12 mM $Tp^{tBuMe}Cu^{II}–OCH_2CF_3$ catalyzed by 1 equiv of TEMPO as monitored by the appearance of $Tp^{tBuMe}Cu^{I}$-MeCN-$d_3$ by $^1$H NMR. The second time course shows the same reaction upon addition of a second equivalent of $Tp^{tBuMe}Cu^{II}–OCH_2CF_3$.

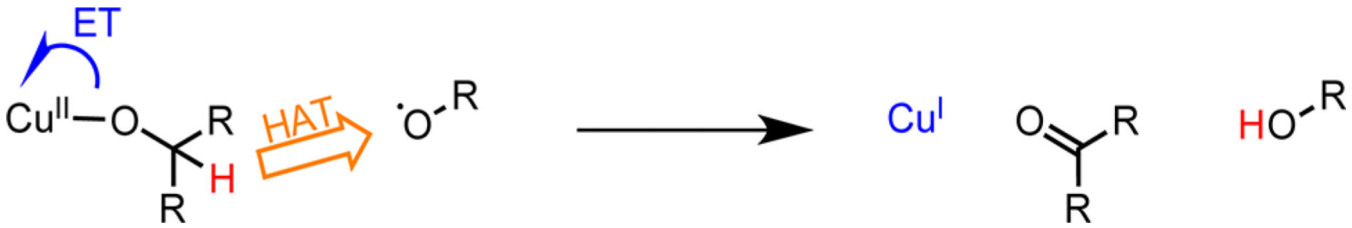


**Scheme 1.**

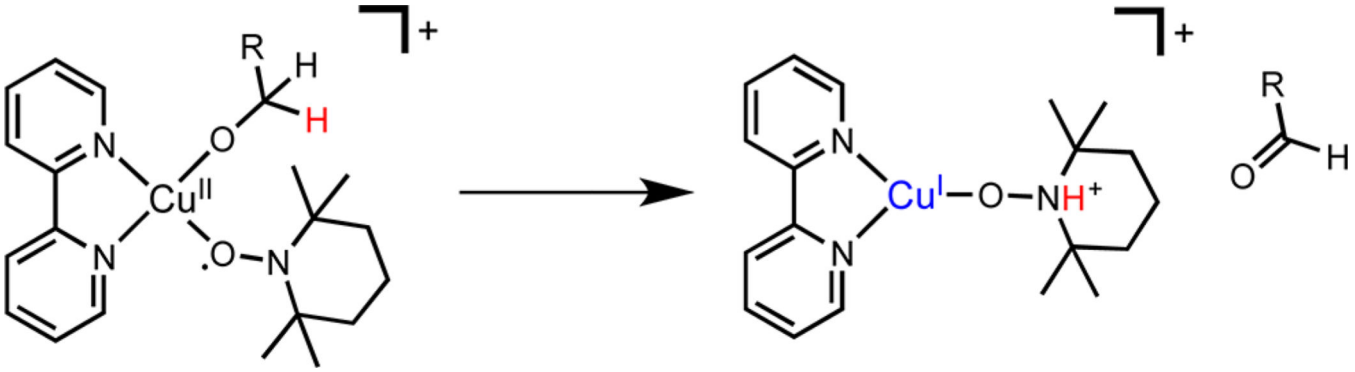


**Scheme 2.**

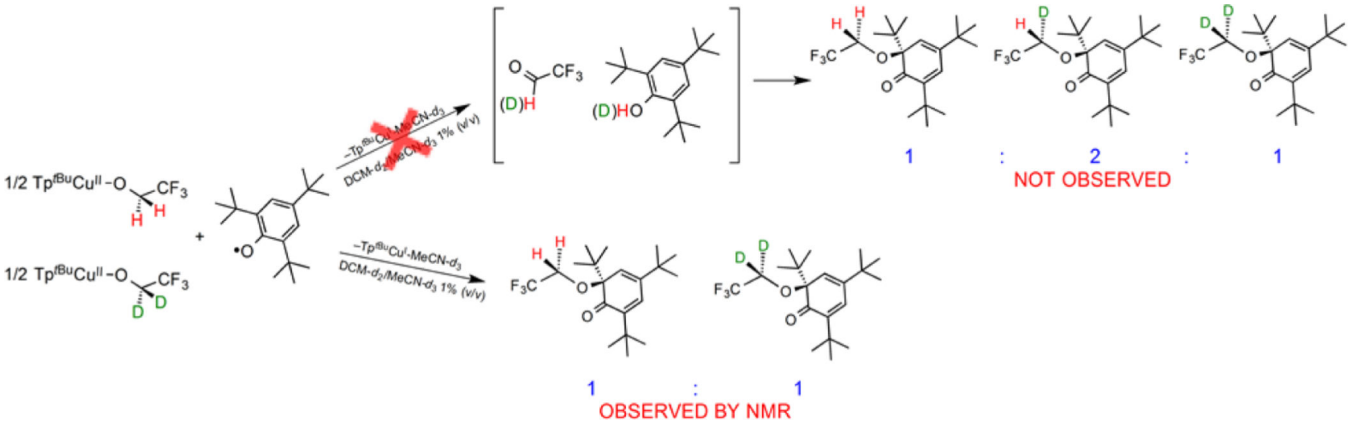


**Scheme 3.**

Trifluoroacetaldehyde and $^{t}Bu_3ArO–H$ Are Not Intermediates in the Reaction between 1 and $^{t}Bu_3ArO^{\bullet}$

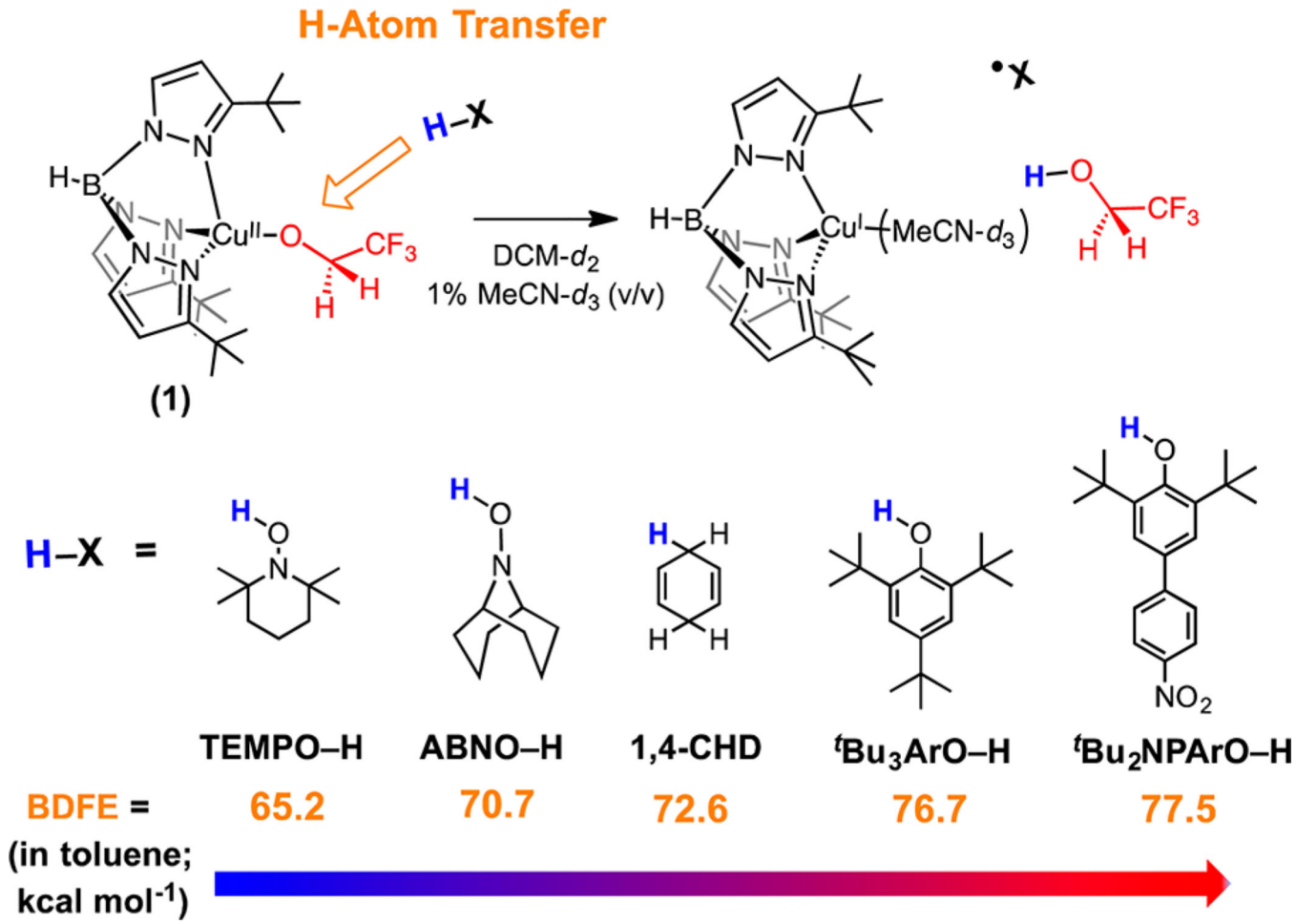


**Scheme 4.**

H-Atom Transfer Reactivitya of 1

[a]For BDFE values, see ref 17.

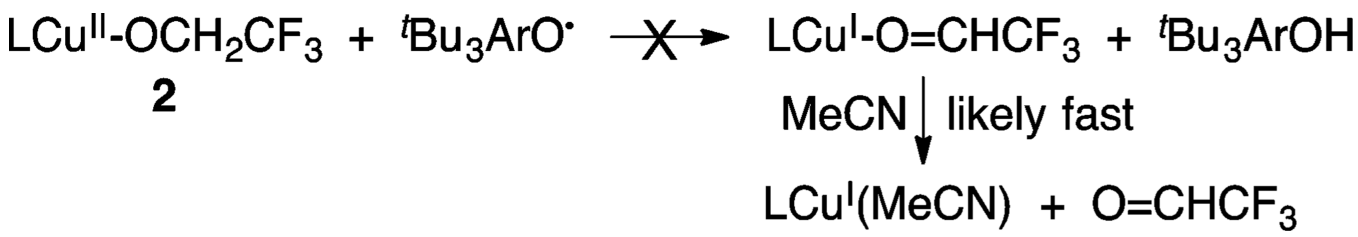


**Scheme 5.**
L = $Tp^{tBuMe}$

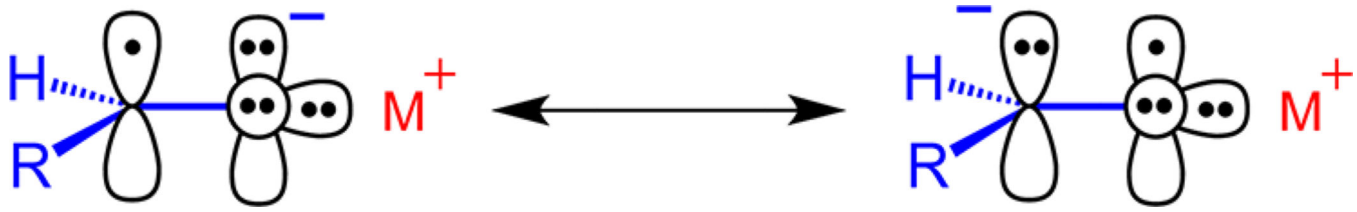


**Scheme 6.**
Resonance Forms for Metal–Ketyl Radical Complexes

**Table 1**

Select Interatomic Distances (Å) and Angles (deg) of 1 and 2

| | 1 | 2 |
|---|---|---|
| | bond | |
| N1–Cu1 | 1.9717(11) | 1.951(2) |
| N2–Cu1 | 1.9638(11) | 1.964(2) |
| N3–Cu1 | 2.2270(11) | 2.230(2) |
| O1–Cu1 | 1.8324(10) | 1.840(2) |
| | angle | |
| N1–Cu1–N2 | 94.21(5) | 93.77(10) |
| N1–Cu1–N3 | 91.15(4) | 91.04(9) |
| N1–Cu1–O1 | 127.18(5) | 133.35(10) |
| N2–Cu1–N3 | 90.92(4) | 91.66(9) |
| N2–Cu1–O1 | 134.28(5) | 128.58(10) |
| N3–Cu1–O1 | 104.96(4) | 104.44(9) |